The EDMS document, containing this report, can be found at the following address: https://edms.cern.ch/document/1688599/1

Acceptance study of the ISOLDE beam lines with MAD-X

E.Rapisarda[1, 2], M.A. Fraser[3], J. Kurcewicz[1], D. Voulot[2, 4]

[1]*CERN, PH Department, CH-1211 Genève 23, Switzerland*
[2]*Paul Scherrer Institut, CH-5232 Villigen PSI, Switzerland*
[3]*CERN, TE Department, CH-1211 Genève 23, Switzerland*
[4]*CERN, BE Department, CH-1211 Genève 23, Switzerland*

C. McGrath[5], V. Karayonchev[6], M. Diem[7]

[5]*Summer Student Programme 2013, Supervisor: J. Kurcewicz*
[6]*Summer Student Programme 2013, Supervisor: E. Rapisarda*
[7]*Summer Student Programme 2014, Supervisors: E. Rapisarda, M. Fraser*

Abstract

A recent survey conducted at ISOLDE has shown that the transfer lines are affected by misalignments that on the vertical direction can, in some points, be as large as 17.4 mm. Such large misalignments surely affect the transport of the beam. The question then arises if the transfer lines need to be realigned in order to improve the beam transmission and shorten the tuning time; the beam tuning at ISOLDE from the merging switchyard in CA0 to the experimental apparatus being a notoriously tedious procedure. This study aims to provide support for the decision to realign. We try to quantify to what extent the steering power available along the transfer line is able to correct the trajectories of the particles and to recover an optimal beam transmission. The beam optics studies have been carried out using the MAD-X programme. MAD-X uses magnetic elements whereas the ISOLDE low-energy transfer lines are made of electrostatics elements. The description of the electrostatic elements of ISOLDE as magnetic elements in MAD-X has been carefully checked throughout extensive SIMION simulations and a good model of the electrostatic transfer lines in MAD-X was obtained. The alignment imperfection of the beam lines have been treated explicitly in the simulation and their distortion effect on the particle trajectories has been corrected using the steering power of the ISOLDE transfer lines.

1. Purpose of the Study

A recent survey conducted at ISOLDE has shown that the low energy transfer lines are affected by significant alignment imperfections especially in the vertical direction.
Figure 1 shows the low energy transfer lines of ISOLDE. The drawing is not up-to-date, in particular the RC4 beam line does not host any device presently (the RF-Spectrometer MISTRAL is dismounted since some years) and it is planned to use this beam line for the new Isolde Decay Station (IDS).
Figure 2 and Figure 3, taken from [1], show the horizontal and vertical offset measured along the transfer line. A detailed description of the measurements performed to determine the actual position of the elements of the ISOLDE beam lines can be found in Ref. [1]. The largest

misalignment of 17.4 mm is measured vertically along the CC0 section. In the text the following notation is used:

Z is the longitudinal dimension, in the direction of the beam
Y is the transversal vertical dimension
X is the transversal horizontal dimension

The imperfection of the transfer lines due to the misalignment introduces trajectory distortions, which finally affect the transmission of the beam to the experimental setup. Steering quadrupole lenses are regularly placed along the low-energy ISOLDE beam lines. The steering quadrupoles combine the steering function of a kicker with the (de)focusing function of a quadrupole.
The aim of this study was to simulate the trajectory distortions introduced by the misalignment and check to what extent these distortions can be corrected by using the available steering power to recover the maximum/optimal transmission along the transfer lines.
The optical transport simulations have been performed by using the MAD-X programme [2]. MAD-X is a general-purpose tool for charged-particle optics design and studies in alternating-gradient accelerators and beam lines. The beam line is defined in MAD-X as a sequence of magnetic elements (dipole magnets, quadrupoles, sextupoles, or multipoles) connected by drift lines. Although the ISOLDE beam lines are made of electrostatic elements, namely quadrupoles, kickers and cylindrical deflectors, which act on the beam through the application of electric fields, the action of the electrostatic elements can be in principle simulated using magnetic elements (the only ones implemented in MAD-X). We have investigated this possibility by carefully comparing the optical behaviour of an electrostatic element with a magnetic element which has an equivalent action on the particle trajectories. The procedure used is as follow.
The particle trajectories in the electrostatic elements were calculated using the 3D tracking code SIMION [3]. SIMION is a software package primarily used to calculate electric fields and the trajectories of charged particles in those fields when given a configuration of electrodes with voltages and particle initial conditions. The elements have been first modelled in CAD software and then imported into SIMION. This allowed us having a very detailed geometrical description of the element in our 3D simulation. Dedicated SIMION scripts were then written to determine (i) the required voltages to be applied to the electrodes for the particle to pass through the element and (ii) to track particles through the element. Another script calculates, out of the many particle trajectories traced through the element, the transfer matrix that represents the action of the given electrostatic element on the particle. The extracted transfer matrices were then compared in MAD-X with the equivalent magnetic transfer matrices. In some cases with the adjustment of few geometrical parameters the optical behaviour of the electrostatic elements can be correctly modelled by the use of the magnetic elements, in other cases the model is approximated and the comparison allowed to identify its limitations.
In Section 2 we will describe in details the modelling of the electrostatic elements in MAD-X. Section 3 is dedicated to the acceptance study while in Section 4 some conclusions will be drawn and plans for further studies will be discussed.

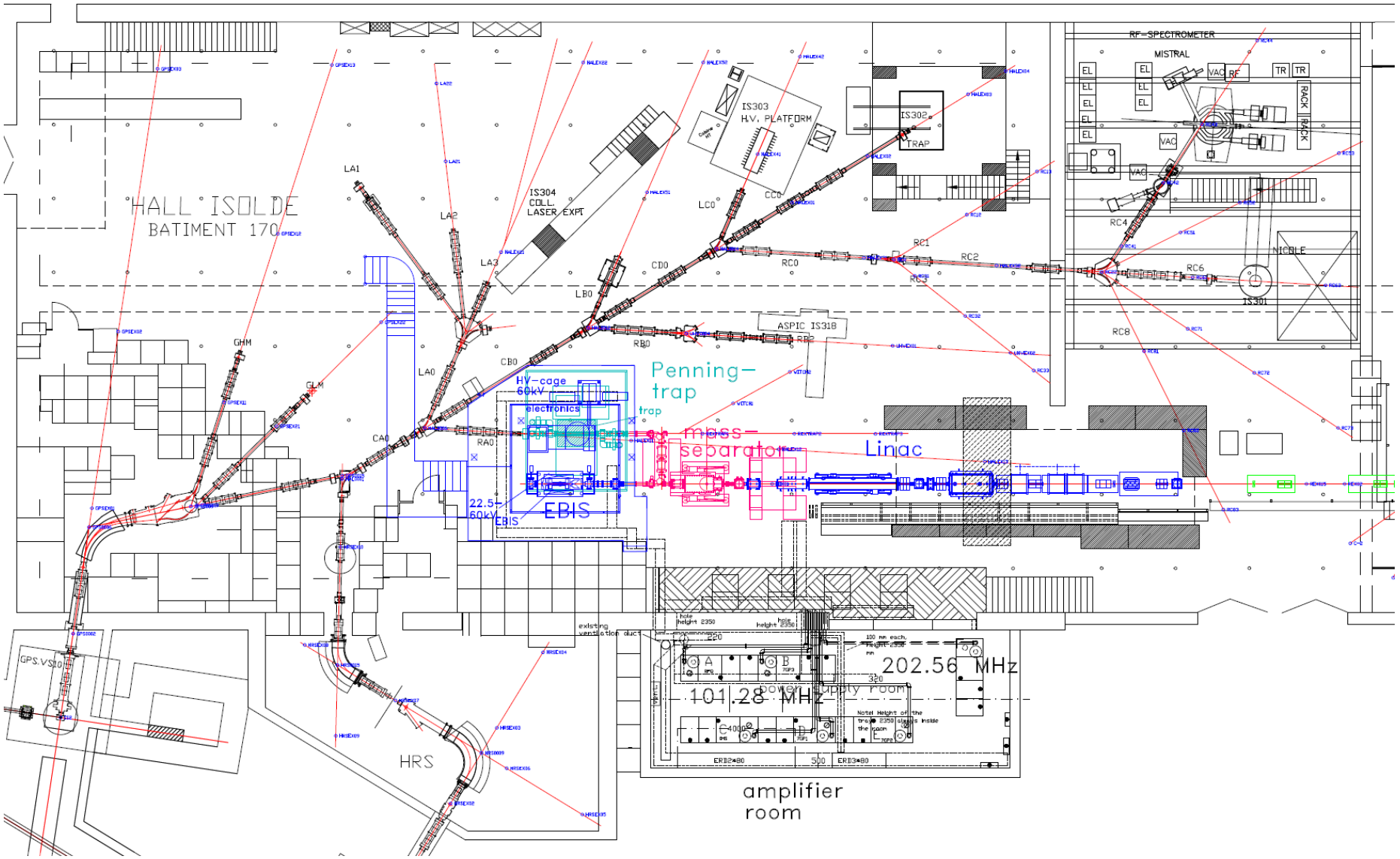

Fig.1 Low energy transfer lines of ISOLDE.

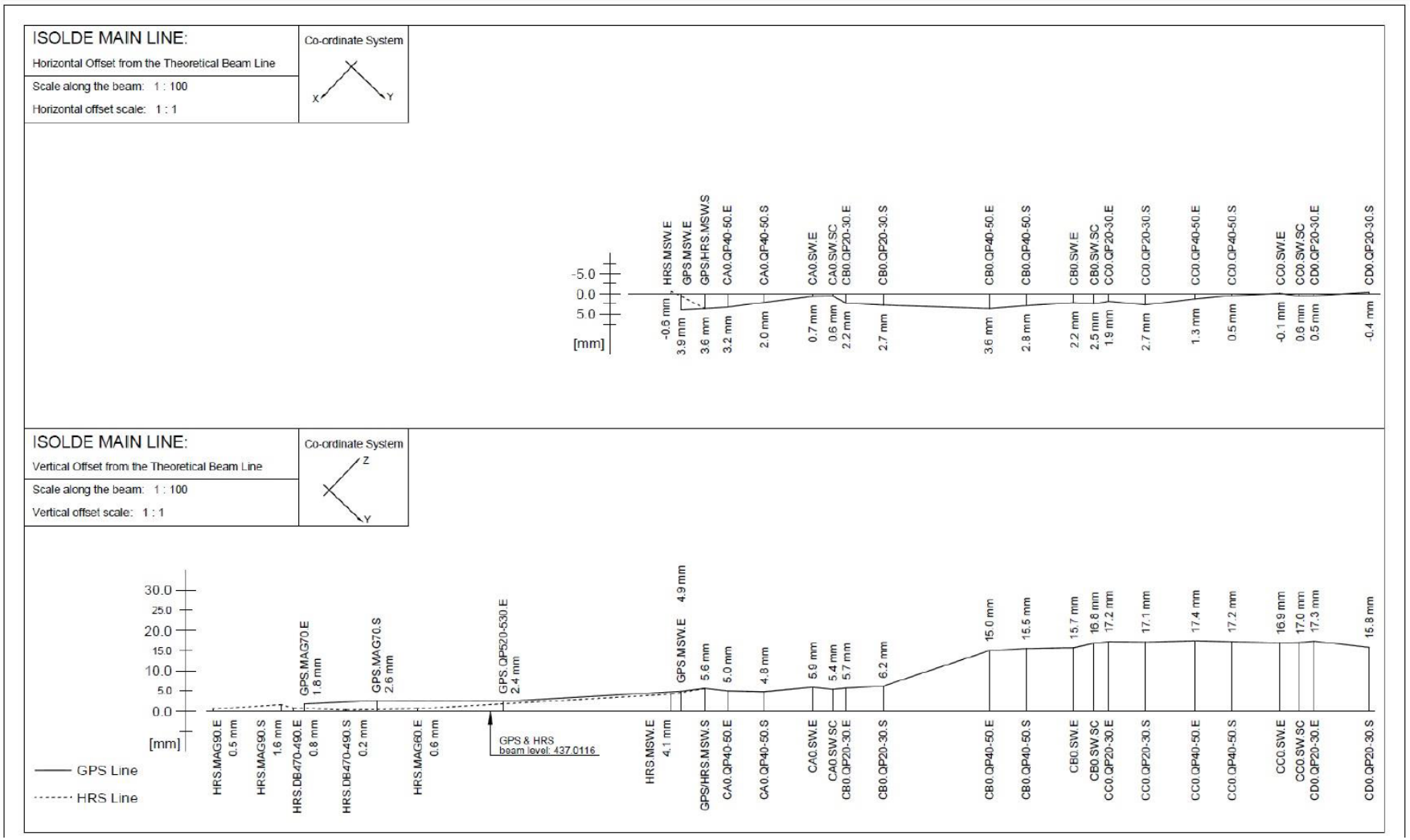

Fig.2 Horizontal and vertical offsets to the theoretical beam lines of HRS, GPS, CAO, CB0, CC0 and CD0 sections [1]

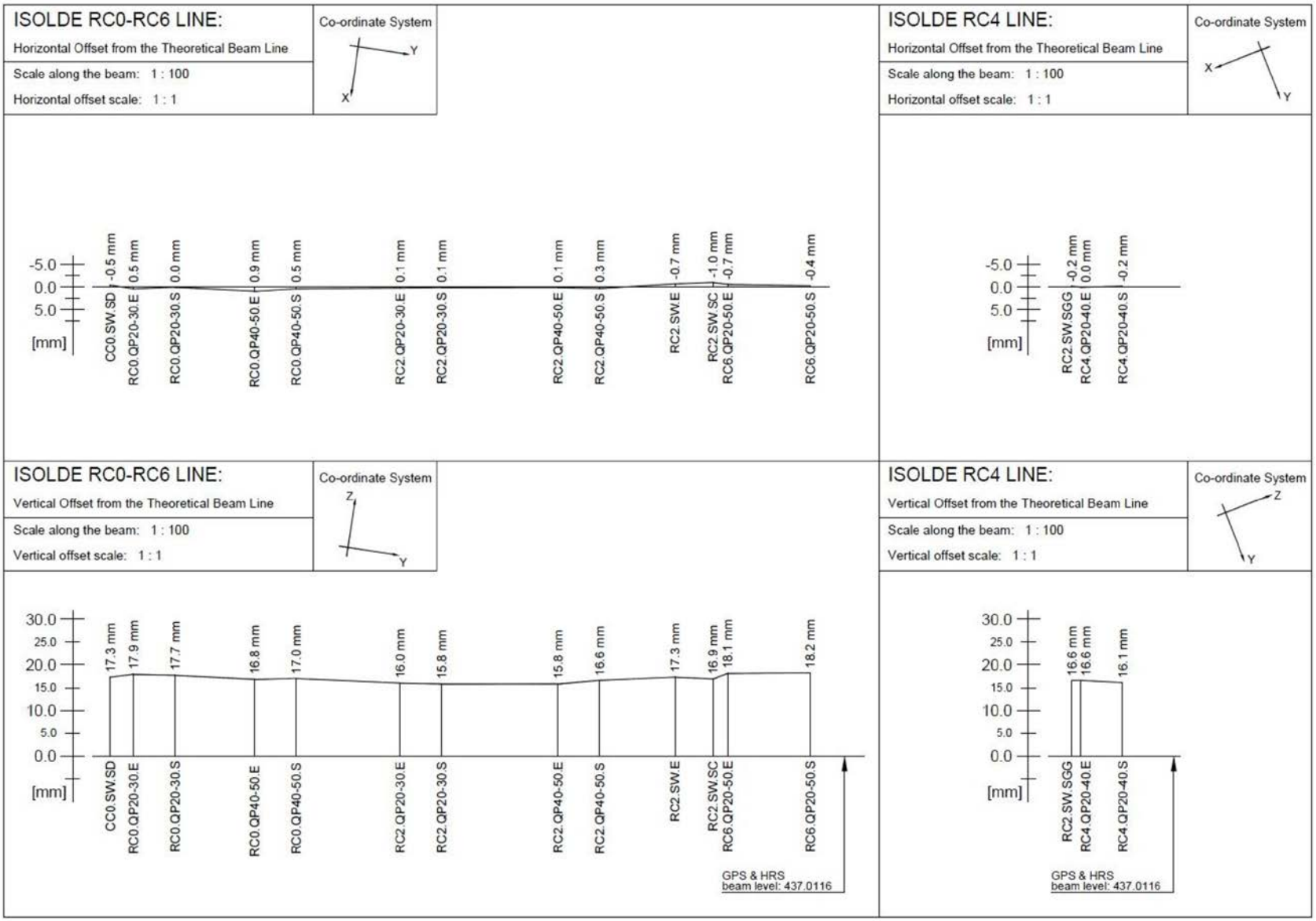

Fig.3 Horizontal and vertical offsets to the theoretical beam lines of RC0, RC2, RC4 and RC6 sections [1]

2. Modelling of the electrostatic elements in MADX

The ISOLDE low energy transfer lines are made of three types of electrostatic elements:

1. Quadrupoles and steering quadrupoles
2. Kickers
3. Switchyards

connected by drift tubes. Some geometrical properties of those elements are listed in Table 1.

Table1: Geometrical properties of the electrostatic elements in the ISOLDE low energy beamlines.

	Electrodes length (mm)	Vacuum chamber (mm)	Aperture type	Aperture opening (mm)
Quadrupole	300	450	Rectangular	Vertical ±70 Horizontal ±70
Kicker	110		Rectangular	Vertical ±55 Horizontal ±20

	Electrodes radius (mm)	Angle (deg)	Aperture type	Aperture opening (mm)
3way-SWY cylindrical deflector	600	27.5	Rectangular	Vertical ±60 Horizontal ±30
5way-SWY cylindrical deflector	600	25,50	Rectangular	Vertical ±60 Horizontal ±30

Quadrupoles are arranged in doublets or triplets. By convention, a focusing quadrupoles is horizontally focusing (and vertically defocusing) and a defocusing quadrupoles is vertically focusing (and horizontally defocusing). Along with quadrupoles, beam steering elements are conventionally incorporated into beamlines. Generally two steerers in each plane (X and Y) together with a quadrupole doublet constitute a module providing full control of the direction, position and focus of the beam. In order to optimize the use of the tight space available for the beam distribution lines, at ISOLDE it was chosen to add the steering elements of the beam line into the quadrupoles. Some quadrupoles, denoted as “steering quadrupoles” have been modified to create a dipole component across the quadrupole. The dipole component is produced by modifying the applied voltage of the opposite electrodes, so that the two opposite electrodes are still receiving the same summed voltage. The steering quadrupole field can also be seen as identical to a regular quadrupole of the same length, physically offset from the centre of the beam line. Hence, the final result is causing the beam to be focused and deflected at the same time towards the new centre of the quadrupole (which does not correspond to the physical centre of the quadrupole) (see Fig.4)

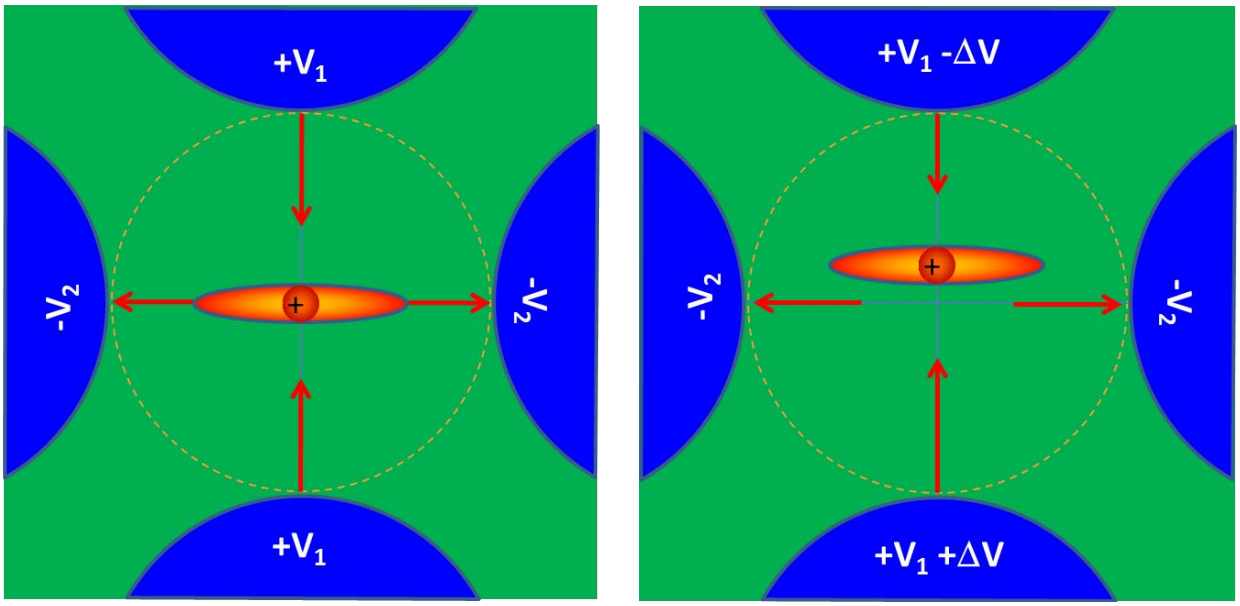

Fig.4. Schematic representation of a balanced quadrupole vertically focusing (left) and the same with a dipole vertical component (right).

The switchyard (SWY) is built up of pairs of electrostatic cylinder- shaped deflector plates, one pair on either side of the central beam line. The switchyard in the beam distribution system serves to transport the ion beam into different beam lines. Two different switchyards exist at ISOLDE: the 3-way SWY which allows to turn the beam to ±27.5 degree direction (Fig.5, right panel) and a 5-way SWY which allows to turn the beam to ±50, ±25 degree (Fig.5, left panel [4]). An electrostatic "kicker", made of two parallel electrostatic plates and placed upstream the switchyard, directs the ions to the entrance of the chosen set of deflector plates, as shown in the CAD drawing of Fig.5, right panel. The entrance axis of the cylindrical deflectors is inclined ±7.5 degree relative to the entrance axis of the kicker in the 3-way SWY and ±5 and ±10 degree in the 5-way SWY. Therefore the total deflection of the beam performed by the SWY-kicker assembly is ±30 degree for the 3-way assembly and ±30, ±60 degree for the 5-way assembly. Since it was not possible to find the technical drawing of the 5-way switchyard, the angles of the kicker and of the deflectors have been estimated from the only available picture (Fig.5, left panel) and from direct measurements of the vacuum chamber of the 5-way switchyard in the beam line.

In order to model the electrostatic element in MAD-X we checked that the action of the electrostatic quadrupoles on the beam is equivalent to the action made by magnetic quadrupoles and that the switchyards act as magnetic benders (SBEND).

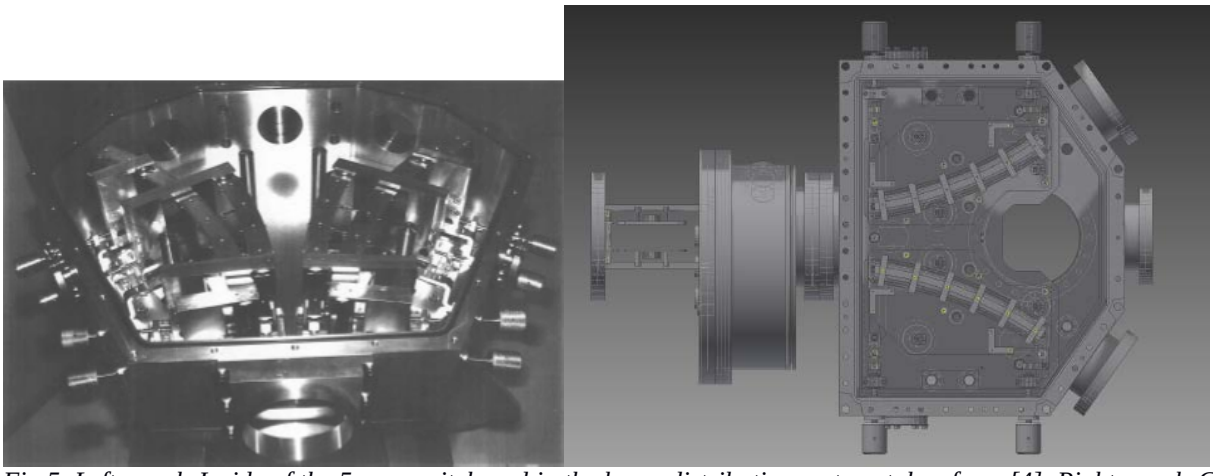

Fig.5. Left panel: Inside of the 5-way switchyard in the beam distribution system, taken from [4]. Right panel: CAD model of the kicker and 3-way SWY assembly used in the ISOLDE beam lines. A diagnostic box is placed between the kicker and the switchyard.

2a. Quadrupole

The optical properties (i.e. focusing/defocusing effect) of an electrostatic quadrupole are expected to be the same as the ones of a magnetic quadrupole. When modelling an electrostatic quadrupole with a magnetic one, the effect of the fringing field can be taken into account by adjusting the length of the magnetic quadrupole in MAD-X to match the tracking results using the realistic fringing electric field.

Figure 6, left panel, shows the CAD drawing of the quadrupole imported in SIMION where the four electrodes and the vacuum chamber are clearly visible.

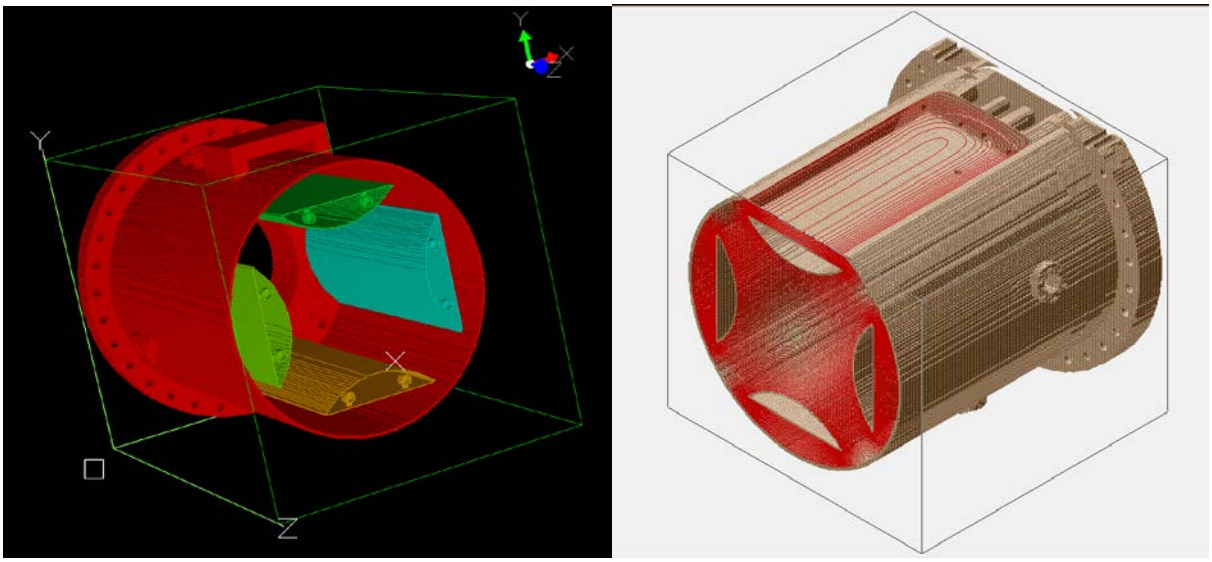

Fig.6. Left panel: Quadrupole 3D-CAD drawing imported in SIMION. Right panel: equipotential lines inside the quadrupole, 3D-view.

Figure 7 shows the equipotential lines of the electric field inside the quadrupole when a given voltage is applied to the electrodes. The electric field does not extend significantly beyond the electrodes, thanks to the design of the shielding electrodes that limit the fringing field. Indeed, the optical matrix of the electrostatic quadrupole is identical within 5% to the matrix of an equivalent magnetic quadrupole of the same length (300mm, see Table 1).

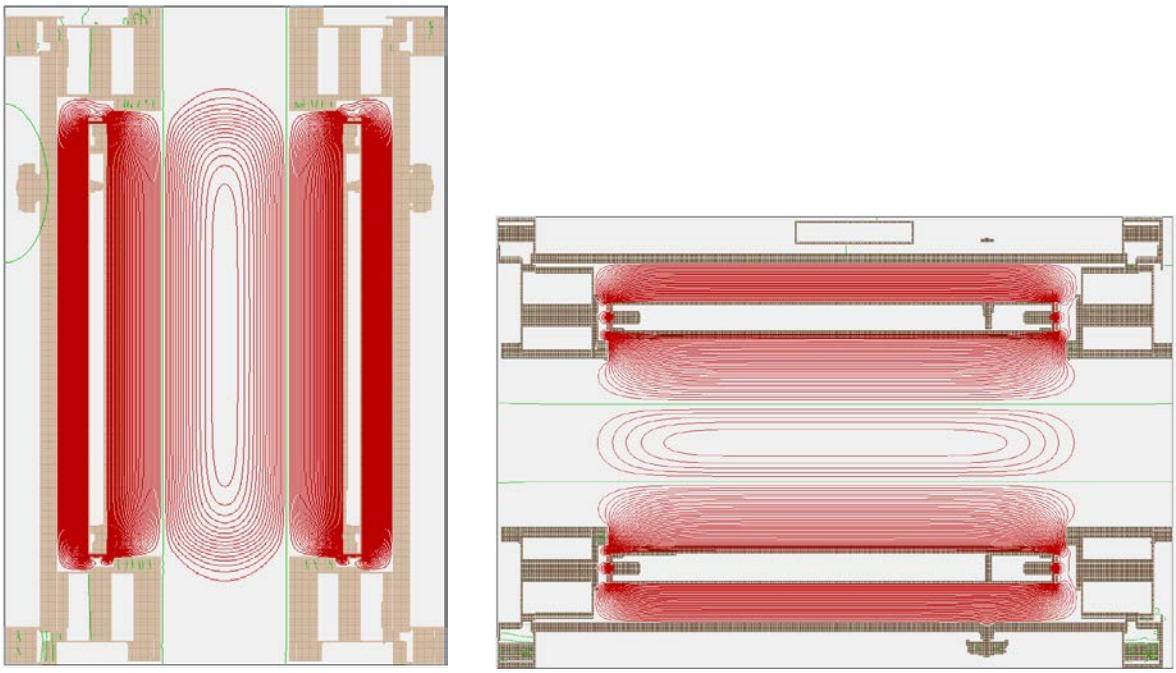

Fig.7: Equipotential lines inside the quadrupole: X-Z view (left panel) and Z-Y view (right panel).

2b. Kicker

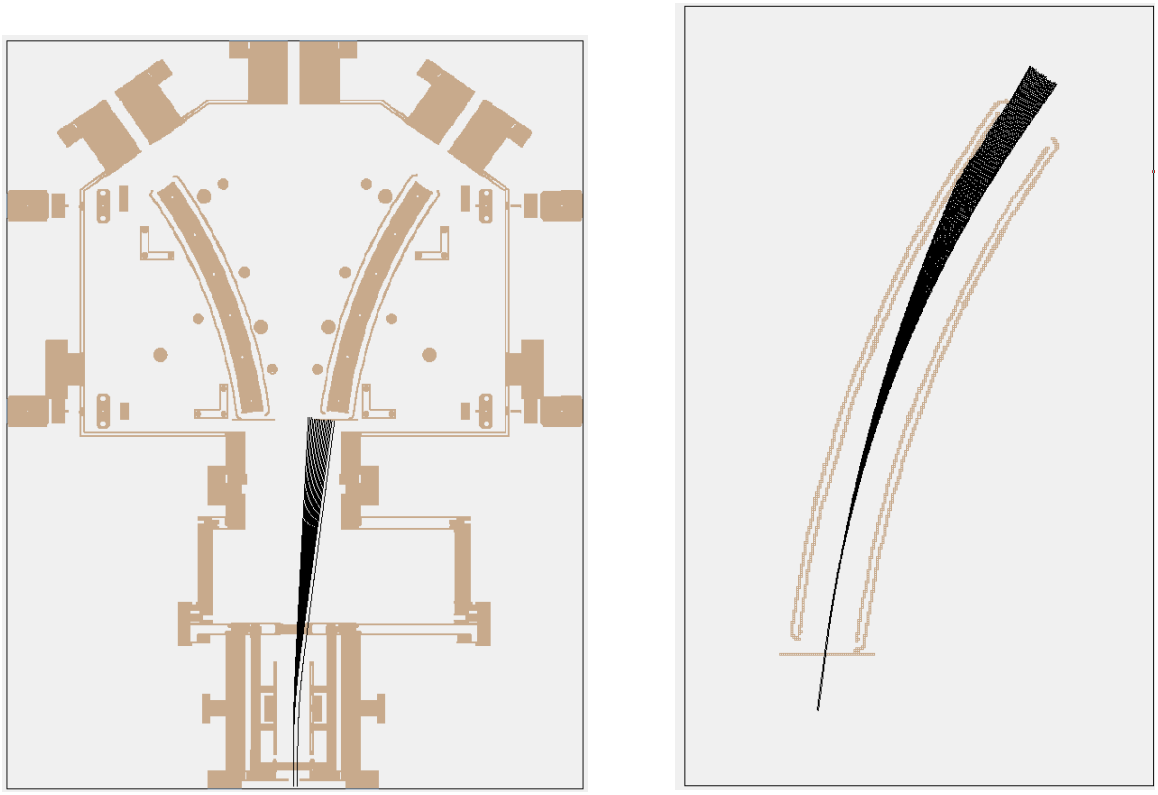

Fig.8: Tracking of particles inside the kicker (left panel) and inside the deflector (right panel) simulated with SIMION for different values of the voltages applied to the electrodes.

The kicker is a component used to direct the ions to the entrance of the deflector. With the same procedure as the one used for the quadrupole, we have tracked particles inside the kicker (see Fig.8, left panel) and calculated the optical matrix (reported in annex 2). The transverse Y optics of the kicker can be very well approximated by a drift, whereas in the transverse X optics the kicker has a slight focusing effect ($R_{21} \neq 0$) compared to the action of a drift. In our MAD-X simulation we have approximated the kicker to a drift, therefore neglecting this effect.

2c. SWY-Deflector

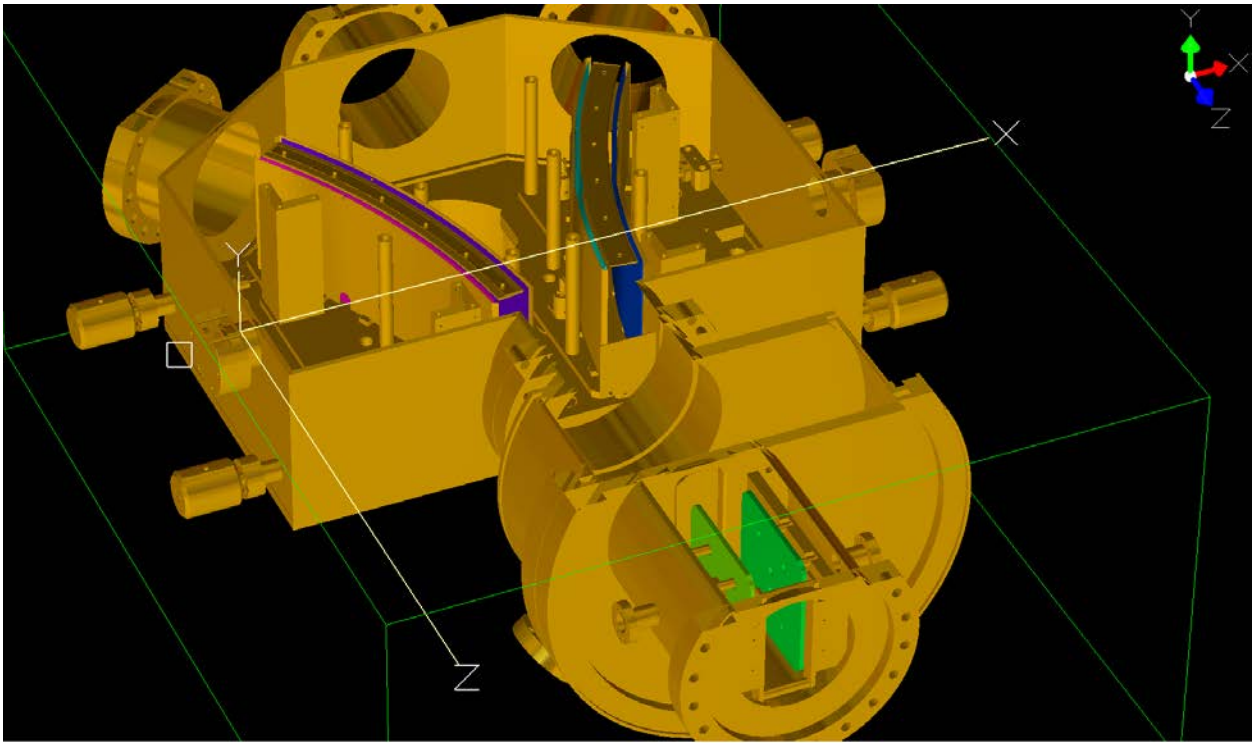

Fig.9: 3D-CAD drawing of the switchyard imported in SIMION. The cylindrical electrostatic deflector plates are clearly visible. The picture also includes the kicker electrodes.

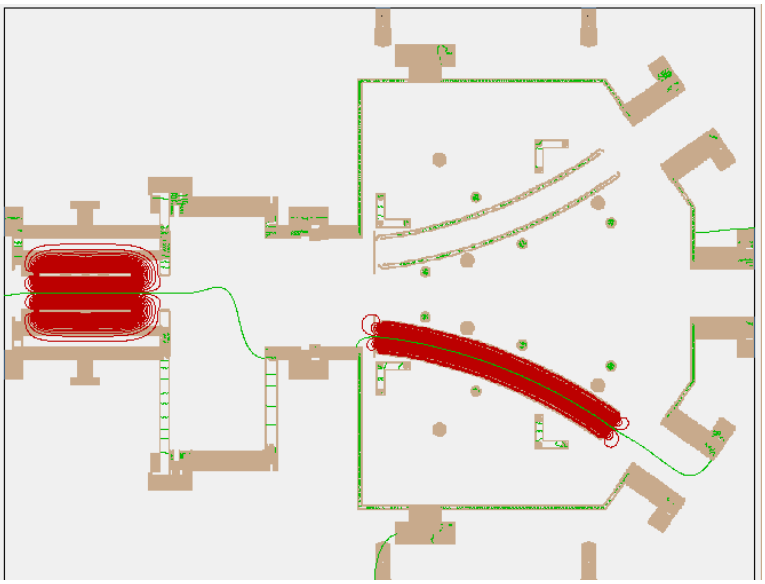

Fig.10: Equipotential lines inside the kicker and the switchyard, Z-X view.

Fig. 9 shows the 3D-CAD drawing of the full assembly kicker and 3-ways switchyard imported in SIMION. Given the vicinity, around 40 cm, of the kicker electrodes and deflector electrodes it is important to check if these elements feel the action of the fringe field of the other. As shown in Fig.10 the equipotential lines of the electric field in the kicker and switchyard assembly are well localized around the corresponding electrodes and no interference is observable.

The particles tracked inside the deflector are shown in Fig.8, right panel.
The action of the switchyard is to redirect the beam. It can be shown that, generally, the optics in the 4-dimensional phase-space (x,x')(y,y') of an electrostatic cylindrical deflector is equivalent to the one of a bending magnet (SBEND in MAD-X) defined by the following parameters:

$$R_{SBEND} = \frac{R_{defl}}{\sqrt{2}} \quad \text{and} \quad \vartheta_{SBEND} = \vartheta_{defl} \cdot \sqrt{2}$$

where R_{SBEND} and ϑ_{SBEND} are the bending radius and angle of the magnet and R_{defl} and ϑ_{defl} are the bending radius and angle of the electrostatic deflector. The path of the reference trajectory inside the magnetic element and the electrostatic element is the same because the factor $\sqrt{2}$ cancels. Of course the reference trajectory resulting from the magnetic element is not realistic but the relative motion about this particle is the same as the electrostatic deflector.
It should also be noticed that the bending magnet matches only the transverse optics of the electrostatic deflector, but the dispersion properties of the electrostatic deflector are not properly reproduced. However, since the typical beam dispersions at ISOLDE are in the order of 10^{-5} [5] the error on the dispersion can be neglected. For precise dispersion studies, or for beams of larger dispersion, our model in MAD-X is not accurate.

2d. Beam line in MAD-X

The beam optics simulations were performed on the beamline going from the beginning of the CA0 beam line to the end of the RC4 beam line. This is one of the longest beam line (around 30 m) present at ISOLDE and has 31 electrostatic elements. In 2013 it was decided to install the new ISOLDE decay station (IDS) at the end of the RC4 beam line and simulations were needed in order to optimize the optics of the last part. It was therefore convenient to combine that study with the study presented in this report on the misalignment of the beamline.
A schematic view of the sequence of elements of the beam line is shown in Fig.11. In the figure, the kickers and the switchyards between the CA0-CB0, CB0-CC0, RC0-RC2 sections are not shown because at those intersections the beam goes straight and therefore in the definition of the sequence, they were simply replaced by drifts. The quadrupoles above the line are horizontal focussing (vertical defocussing) and according to the convention in MAD-X they have a positive quadrupole strength. The quadrupole below the line are horizontal defocussing (vertical focusing). The dashed elements indicate the monitors.

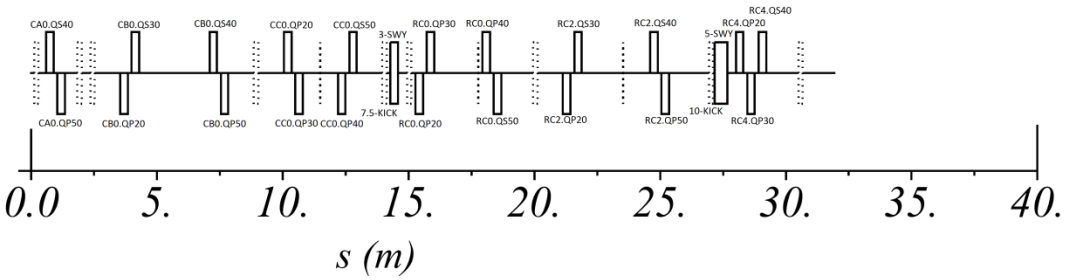

Fig.11: Schematic view of the simulated beam line showing the position of the quadrupoles (QP), steering quadrupoles (QS), kickers (KICK) and switchyards (SWY). The dashed lines show the position of the monitors.

3. Acceptance Studies

Once we had achieved a suitable modelling of the ISOLDE transfer lines in MAD-X, the study of the effect of the misalignment on the beam transport and of the possible corrections of the beam orbits was addressed.

The initial beam optical properties at ISOLDE are difficult to define due to the different types of target-ion sources (surface ionizing, plasma, RILIS) and the different ion-source parameters. In order to overcome this issue, the study of the beam transmission has been conducted in terms of a phase-space acceptance study. The initial beam conditions were extracted according to a uniform distribution in the horizontal (x,x') and vertical (y,y') transverse phase-space. The phase-space was chosen large enough to cover the typical emittances of the ion-sources at ISOLDE [6]. After tracking of the particles in the beam lines, the acceptance is calculated by measuring the fraction of the initial phase-space corresponding to ions which have been transmitted through the beam line, according to the aperture of the elements including their misalignment. The tracking of each particle is done using the TWISS module [2] available in MAD-X.

The nominal optics of the transport line from the CA0 merging switchyard to the end of the RC4 beam line was taken from an experimental setting reported in annex 1 and scaled to 50 keV. The quadrupole strength K to be applied to the magnetic quadrupoles was calculated from the voltages using the formula

$$K = \frac{2 \cdot V_0}{R_0^2} \cdot \frac{q}{m \cdot \gamma \cdot \beta^2 \cdot c^2}$$

where R_0 is the distance of the quadrupole electrode to the centre of the quadrupole and V_0 is the applied voltage. The steering power was neglected. The β-functions corresponding to this experimental setting were calculated in MAD-X and are shown in Fig.12.

The experimental setting we have used does not correspond to the best tuning of the beam line. This setting was indeed one of the first attempts to transport the beam to the end of RC4 line after several years the beam line was not in use. With this setting the transmission from the GPS.FC5580 to RC4.FC0900 was only 52%. We aim to stress here that the study we are going to present is a relative estimation of the acceptance of the misaligned beam line.

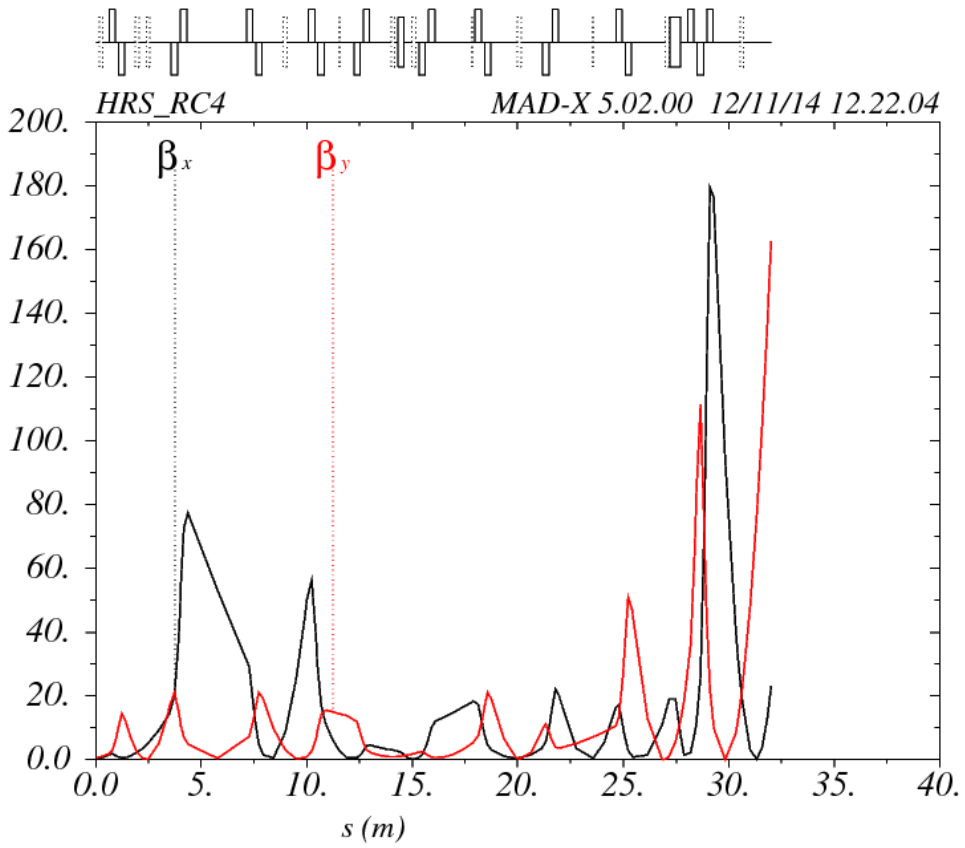

Fig.12: Nominal optics of the CA0, CB0, CC0, RC0, RC2, and RC4 beam line: β-functions.

In order to quantify the effect of the misalignment, three acceptance studies are carried out:

1. theoretical beam line, no misalignments included;
2. including misalignments as measured from the survey → generating optics and trajectories (distorted);
3. correcting trajectories and recalculating the optics

From the relative ratio of the acceptances calculate in case 1) and 3) we estimate the effectiveness of the steering power.

3a. Theoretical, perfectly aligned transfer lines

Figure 13 shows the injected (left) and accepted (right) (x,x') and (y,y') phase-space.
Due to the fact that the vertical apertures of the elements are larger than the horizontal ones, the injected phase-space was chosen ±15mrad in x' and ± 5.0 mm in x and ±15mrad in y' and ± 10.0 mm in y. The area of the transmitted phase-space is around 27π (mm mrad) in (x,x') and 90π (mm mrad) in (y,y'). This study provides an estimation of the maximum emittance that can be transported along the ISOLDE beam lines (aligned). The beam line acceptance in the horizontal phase-space is a factor two larger than the emittances measured in Ref.[6] for different ISOLDE ion sources. Since the experimental setting we used was not optimized, the acceptance of the beam line can be even larger.

Figure 14 and Figure 16 show, respectively, the horizontal and vertical trajectories of the particles emitted in the (x,x') and (y,y') injected phase-spaces. The black lines correspond to the apertures of the quadrupoles, kickers and deflectors. From the inspection of the beam envelope, one can clearly see that the X transverse optics was not well matched to the beam line in correspondence of the intersections CB0-CC0 and RC2-RC4.

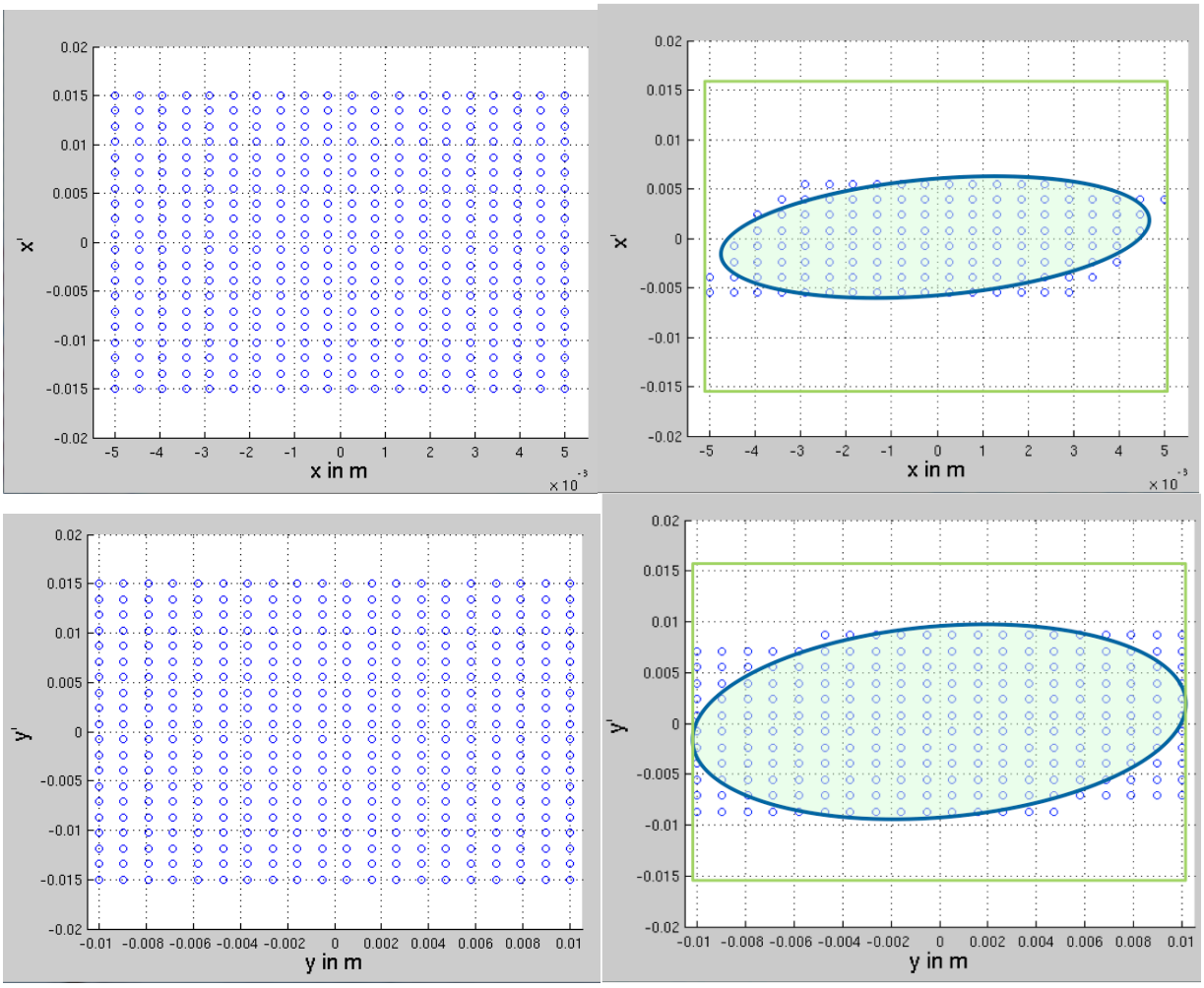

Fig.13: Left side: injected (x,x') (top) and (y,y') (bottom) phase-space. Right side: accepted (x,x') (top) and (y,y') (bottom) phase-space for a perfectly aligned beam line.

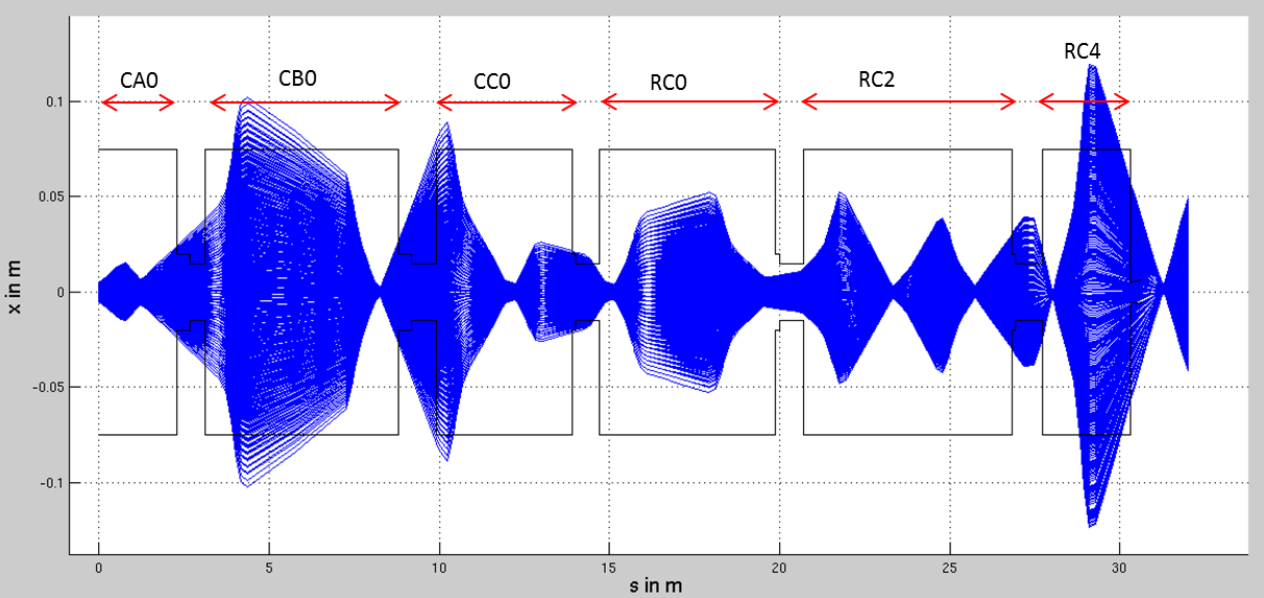

Fig.14: Trajectories in the X-plane calculated with the TWISS module for a perfectly aligned beam line.

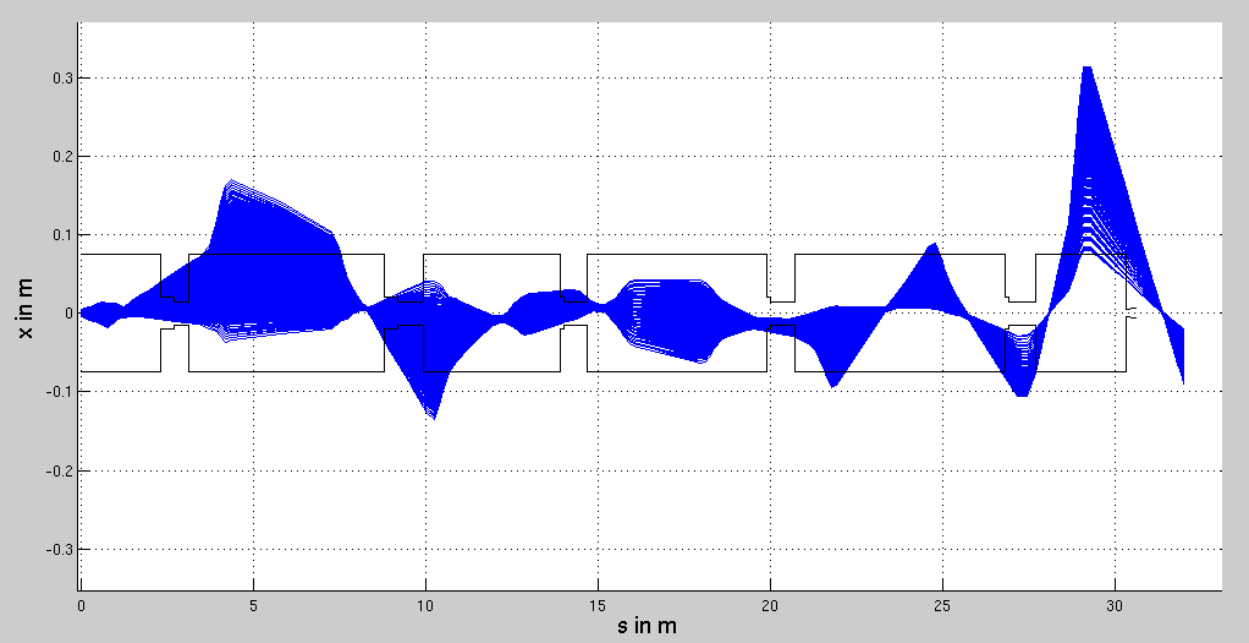

Fig.15: Trajectories in the X-plane calculated with the TWISS module for the misaligned beam line.

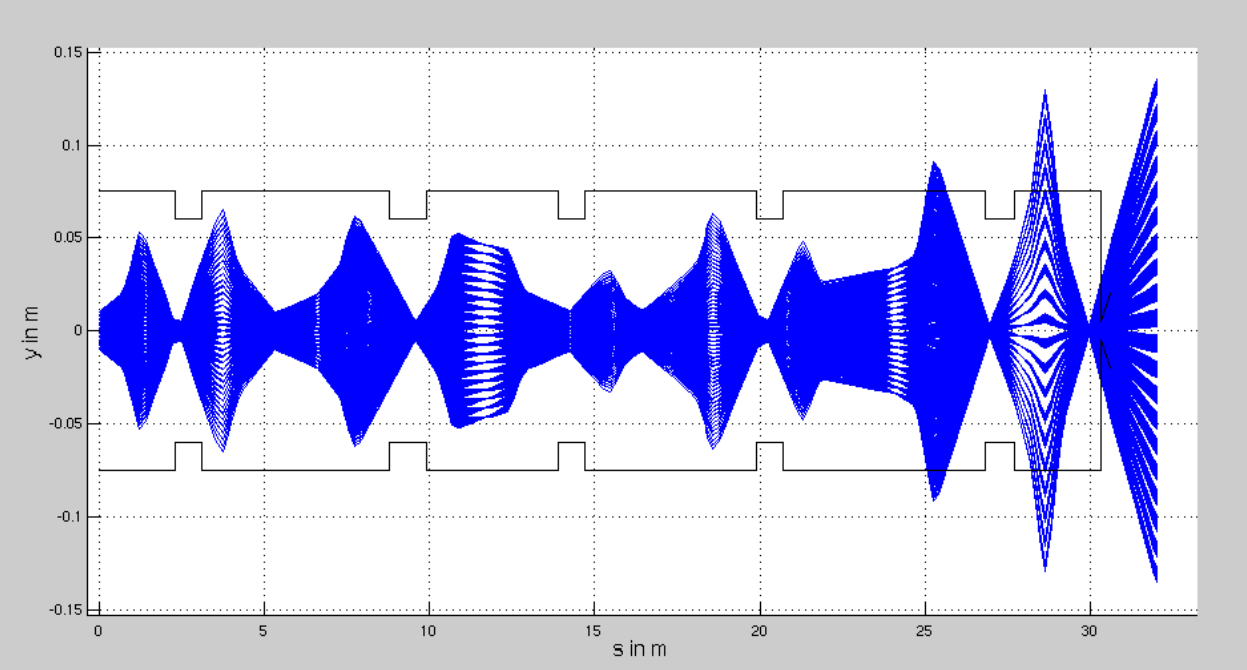

Fig.16: Trajectories in the Y-plane calculated with the TWISS module for a perfectly aligned beam line.

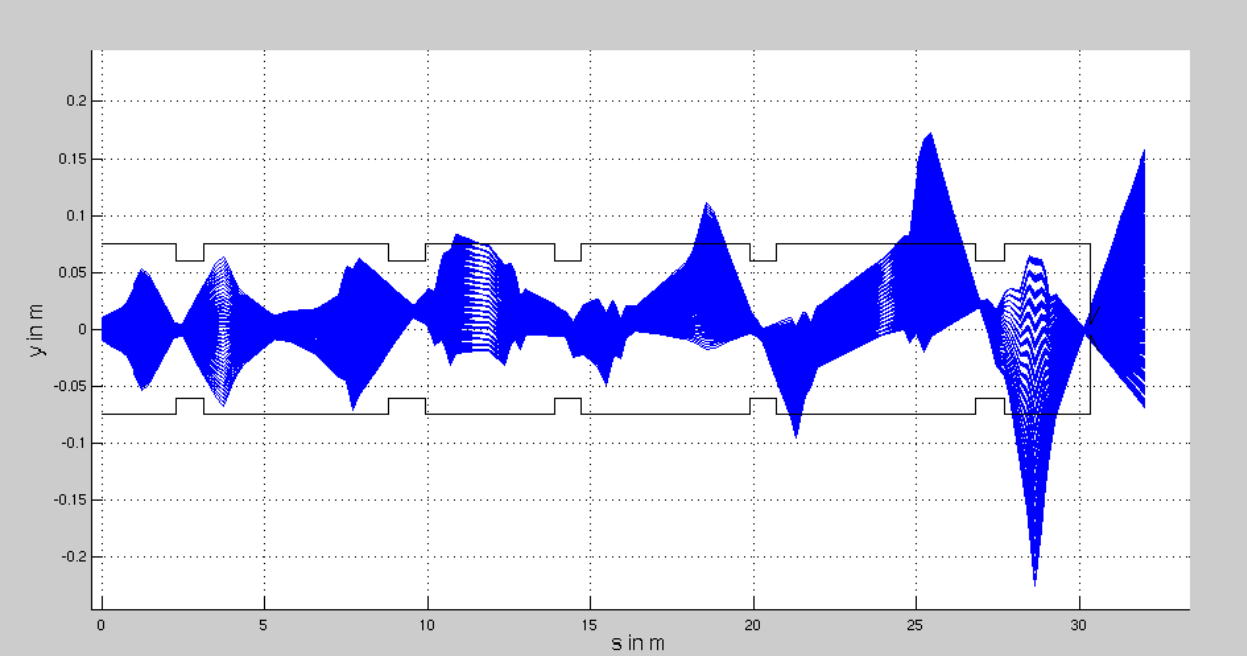

Fig.17: Trajectories in the Y-plane calculated with the TWISS module for the misaligned beam line.

3b. Misaligned transfer line and distorted trajectories.

In the second step of the beam acceptance study we assigned an alignment error, in X and Y, to the elements of the beam line, according to the displacement of the position measured in the survey (see Fig. 2 and Fig.3) and the optics and the trajectories of the particles were generated

for the misaligned transfer line. Since the beam line simulated in MAD-X starts from the exit of the CA0 merging switchyard, the vertical errors assigned to the elements correspond to their vertical displacement taking as zero the vertical displacement of the GPS.MSWE, i.e. they were reduced by 4.9 mm (see Fig.2).
Figure 15 and Figure 17 show, respectively, the horizontal and vertical trajectories of the particles emitted in the (x,x') and (y,y') injected phase-space when the beam line is misaligned. The apertures of the quadrupoles, kickers and deflectors are indicated by the black lines. The plot shows that the effect of the misalignment on the trajectories is such that none of the particles in the injected (x,x') phase-space can be transmitted through the misaligned transfer line.

3c. Correction of the trajectories

The final step of this work is to correct the trajectories distorted by the misaligned beam lines. The possibility to correct a trajectory is a built-in functionality in MAD-X. Beam monitors were defined at the position of the diagnostic boxes and correctors were defined at the position of the steering quadrupoles. A total of 8 horizontal and vertical steering quadrupoles are present along the ISOLDE transfer line subject of the present study. The action of a corrector is to kick the beam, horizontally or vertically. The strength of a trajectory corrector is the deflection angle and is measured in rad. The trajectory correcting algorithm minimizes the trajectory distortions at the monitors by kicking the beam.
A global correction was performed using the MICADO correcting algorithm. The result of the trajectory correction is reported in Table 2 (horizontal corrections) and Table 3 (vertical corrections). From the deflection angles, the corresponding voltages were then calculated assuming a beam energy of 50 keV. These voltages are also reported in Table 2 and Table 3 and fit well within the range of the power supplies (+/- 300V) of the steering quadrupoles although in some cases they are close to their limit (RC2.QS40).

Table 2. Horizontal corrections.

Steering Quadrupole	Deflecting angle (mrad)	Voltage (V)
CA0.QS40	-5.80	-68
CB0.QS30	-2.72	-32
CC0.QS50	0.67	8
RC0.QS40	0.31	4
RC2.QS40	0.17	2
RC4.QS40	-0.48	-5.6

Table 3.Vertical corrections.

Steering Quadrupole	Deflecting angle (mrad)	Voltage (V)
CA0.QS40	-1.53	-18
CB0.QS30	1.98	23
CC0.QS50	0.56	6.6
RC0.QS40	10.0	117
RC2.QS40	-22.9	-268
RC4.QS40	-13.3	-156

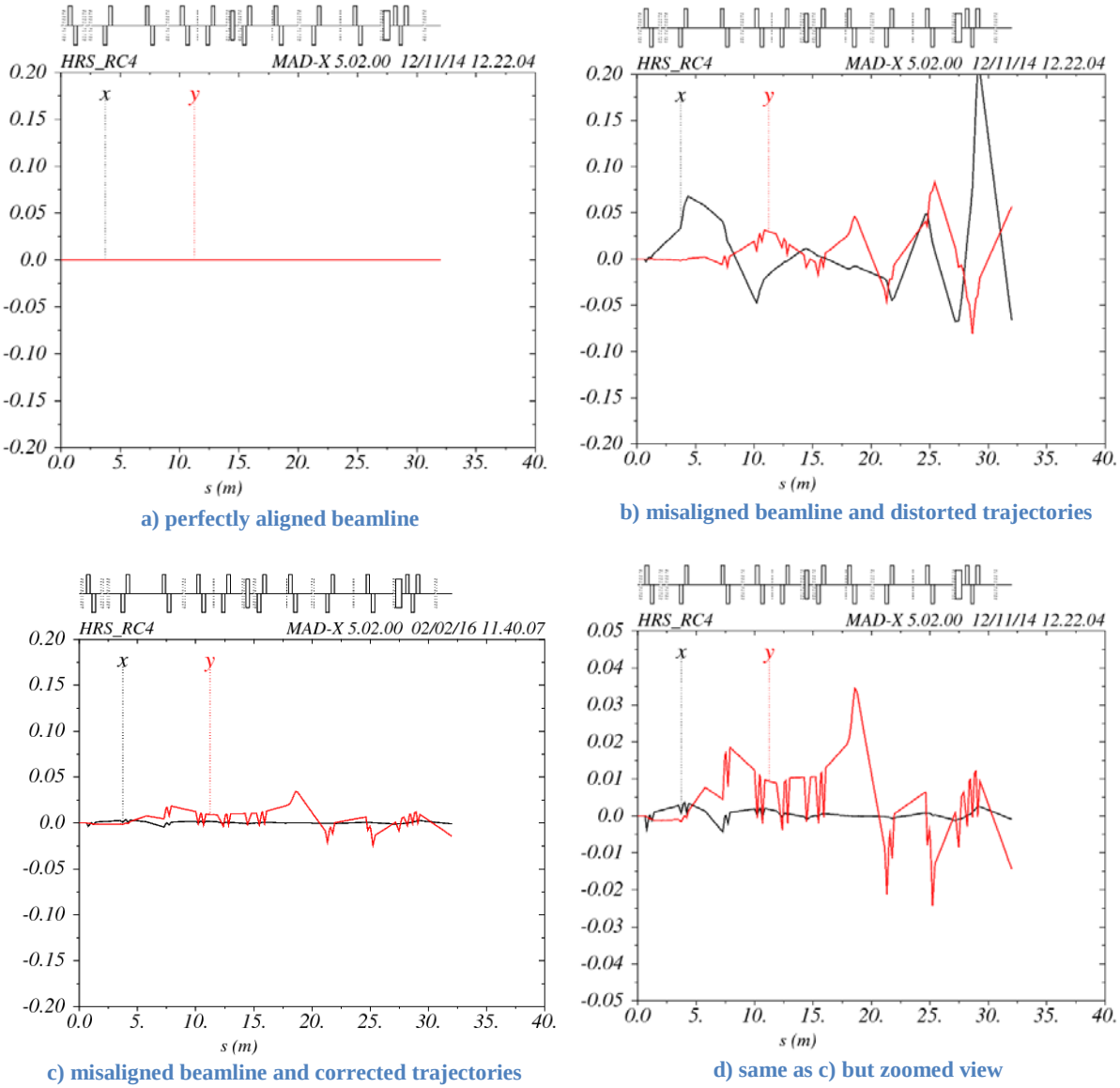

Fig.18: X and Y reference trajectories (in m) for the three studied cases.

Figure 18 shows the reference trajectories in X and Y for the three studied cases: a) perfectly aligned transfer line, b) misaligned transfer line and distorted trajectories, c) and d) misaligned transfer line and corrected trajectories. As shown in figure 18-c) and d) the distortion on the trajectories can be quite well recovered on the X direction and to a large extent also on the Y direction. The comparison of the plot a) and d) in Fig.18 shows that the corrected horizontal reference trajectory (d) in the misaligned beam line is displaced by less than 5 mm with respect to the horizontal reference trajectory in the perfectly aligned beam line (a). On the other hand, the corrected vertical reference trajectory shows a larger displacement up to 3.5 cm. To better quantify the effect of the displacement of the reference trajectory, we start from the same injected phase-space as Fig.13 left panel and we calculate the accepted phase-spaces in the (x,x') and (y,y') planes. These are shown in Fig. 19. They are comparable with the accepted phase-space calculated in the case of a perfectly aligned transfer line, showing that the correction

applied to the particle trajectories through the steering quadrupoles is sufficient to recover the same transmission as the one of a perfectly aligned beam line. This result is due to the fact the major misalignment is in the vertical direction where also the apertures of the electrostatic elements (kicker and deflector) are larger compared to the horizontal ones. If the misalignments were in the horizontal direction, it would be more difficult to recover a good transmission.

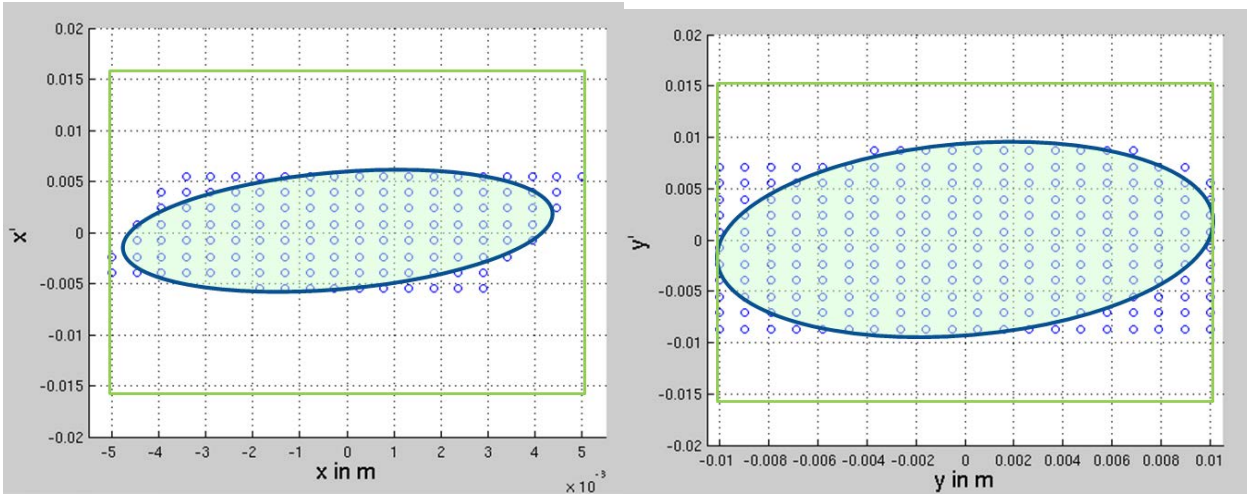

Fig.19: Accepted (x,x') (left panel) and (y,y') (right panel) phase-space for the misaligned transfer line with corrected trajectories.

4. Conclusions

At this point the ISOLDE low-energy transfer lines have been modelled in MAD-X and the transmission of a sampled phase-space through the transfer line has been simulated.
The alignment imperfections have been explicitly treated in MAD-X and a trajectory correction has been performed. The result of this study shows that the transmission of the transfer lines can be recovered by using the correction power of the available steering quadrupoles. This is a rather fortunate situation because a misalignment in the horizontal direction would have been more difficult to handle due to the fact that the horizontal apertures of the elements are smaller.
Practically, after a very long tuning procedure which can take up to 8h, one could achieve a transmission to RC4 of around 80% to 90%. This somehow confirms our results that, thanks to the steering present in the beamlines, the beam can be tuned also in to a misaligned beam line. The decision to realign the beamline should therefore be taken just in consideration of the long time required to optimize the beam line settings. The large misalignment makes it difficult to tune the beam because each quadrupole adjustment has a steering effect on the beam as it is not always well centered. One could indeed expect that a well aligned beam line would simplify the tuning procedure and that once the optimal tuning is found, it can be applied to different ion sources or separator settings (this is not the case at present, as every new beam extracted from the target needs a new transport setting). Very recently Tim Giles and collaborators have developed an automatic beam optimizer that performs the tuning procedure in place of the users but the procedure is still as long as the one manually done by the users.
These simulations could be extended in a future work, by adding the GPS section and the HRS section (downstream the ISCOOL). This would allow a better modelling of the initial phase-space. The contribution from different error sources other than the alignment imperfections of the transfer line,

like power supply ripples, rotation of the electrostatic poles inside the vacuum chamber could also be introduced in order to improve the simulations.
As a next step we would like to apply the calculated corrections to different experimental settings in order to quantitatively estimate the possible improvement of the optical transmission and beam quality. It is the first time that simulations of the low-energy beam line of ISOLDE were performed in MAD-X. Now that the optical matching of the electrostatic and magnetic elements has been checked and optimized, other ISOLDE beam lines can be easily defined in MAD-X and the optics simulated. This is a very useful tool when one would like to optimize some part of a beam line for example in the aim to match better the optics to a new experimental setup.

5. Acknowledgements

We would like to thank Daniel Barna from the TE Department for the useful discussion and his great help with the SIMION scripts. We also gratefully acknowledge Tomasz Wlodarski, student at AGH University of Science and Technology in Krakow for his work in producing the CAD drawings of beam line elements.

6. References

[1] M. Boruchowski et al., https://edms.cern.ch/document/1281872, March 2013
[2] MAD-X web-page: http://madx.web.cern.ch/madx/
[3] SIMION web-page: http://simion.com
[4] E. Kugler, Hyperfine Interaction 129 (2000) 23
[5] A. Jokinen et al. Nuclear Instrument Methods B204 (2003)86
[6] F. Wenander *et al.*, Nucl. Instr. Meth. B204 (2003) 261

7. Material:

Survey: G:\Departments\AB\Projects\REX\REXLinac\Survey

Beamline Drawings :
CERN Drawings Directory, https://edms5.cern.ch/cdd/plsql/c4w.get_in
Direct Drawing Retrieval
CERN drawing number : ISLLSHIR%

ANNEX 1

Voltages of the elements of the beam line from HRS to RC4. These voltages have been taken from a beam tuning done on 2014/08/22 03:59 for a beam of 29.88 keV and have been scaled to 50 keV.

(GPS elog entry 21-08-2014 at 04:12)

```
hrs.qp30 =       -1752.64;
hrs.qp40 =       1385.01;
hrs.qp50 =      -2269.85;
hrs.qp170 =       -1232.81;
hrs.qp180 =       1850.19;
hrs.qp330 =      -948.96;
hrs.qp540 =              0;
hrs.qp550 =              0;
hrs.qp640 =      -146.78;
hrs.qp720 =      -5459.06;
hrs.qs730 =       11610.87;
hrs.qp740 =       -5457.67;
hrs.qp820 =       -5932.47;
hrs.qs830 =       6971.97;
hrs.qp840 =      -1059.63;
CA0.KI10 =     2367.80;
CA0.QS40 =     2242.30;
CA0.QS40H =              0;
CA0.QS40V =              0;
CA0.QP50 =     -2125.17;
CA0.DE60 =               0;
CA0.KI70 =               0;
CB0.QP20 =     -1644.91;
CB0.QS30 =     1156.29;
CB0.QS30H =              0;
CB0.QS30V =    -117.14;
CB0.QS40 =     1055.39;
CB0.QS40H =              0;
CB0.QS40V =              0;
CB0.QP50 =     -1390.56;
CB0.KI70 =               0;
CC0.QP20 =     1469.21;
CC0.QP30 =     -1266.73;
CC0.QP40 =     -1005.69;
CC0.QS50 =     1581.33;
CC0.QS50H =              0;
CC0.QS50V =              0;
CC0.KI70 =     2264.06;
RC0.BE10 =     2388.39;
RC0.QP20 =     -1494.65;
RC0.QP30 =     1171.85;
RC0.QP40 =     1162.48;
RC0.QS50 =     -1497.82;
RC0.QS50H =              0;
RC0.QS50V =              0;
RC0.KI70 =               0;
RC2.QP20 =     -1774.10;
```

RC2.QS30 = 1733.10;
RC2.QS30H = 0;
RC2.QS30V = 0;
RC2.QS40 = 1979.75;
RC2.QS40H = 0;
RC2.QS40V = 0;
RC2.QP50 = -1672.02;
RC2.KI70 = 3835.34;
RC4.BE10 = 2489.96;
RC4.QP20 = 1189.76;
RC4.QP30 = -2409.64;
RC4.QS40 = 1815.60;
RC4.QS40H = 66.93;
RC4.QS40V = 100.40;

ANNEX 2

KICKER MATRIX extracted from the 3D SIMION simulation (2000 particle traces)

0.916884	0.405004	0.002004	0.003380
-0.243770	0.977148	0.003485	-0.000924
0.000665	0.004225	0.997977	0.435403
0.002923	0.011520	-0.006775	0.997002